Vibrational and rotational effects on the intersystem crossing in pyrazine and pyrimidine

Paul Uijt de Haag and W. Leo Meerts

Fysisch Laboratorium, University of Nijmegen, Toernooiveld, 6525 ED Nijmegen, The Netherlands

We have measured the laser induced fluorescence spectra of the $6a_0^1$ and the $6b_0^2$ vibronic bands of the $S_1 \leftarrow S_0$ electronic transition in pyrimidine as well as the $6a_0^1$ vibronic band of the $S_1 \leftarrow S_0$ electronic transition in pyrazine. The instrumental line width of 12 MHz allowed the recording of rotationally resolved spectra. Each rotational transition consists of a group of lines due to the coupling of the excited singlet state to background triplet states. The rotational constants of the S_1 $6a^1$ and the S_1 $6b^2$ states in pyrimidine were determined. Using the standard deconvolution method the singlet–triplet coupling constants and the density of coupled states are derived for several excited rotational states in both bands. The result shows that the intersystem crossing in pyrimidine is independent of the rotational quantum numbers up to $J' = 4$. Comparison with the 0_0^0 vibronic band shows an absence of a strong vibrational effect on the intersystem crossing. We have also applied the deconvolution method on the P(1)-branch of the $6a_0^1$ vibronic band of pyrazine. The density of background triplet states is increased with a factor of 2.4, in good agreement with the calculated increase in the density of states. Except for a minor diminution of the average coupling matrix element no vibrational effect on the intersystem crossing was found.

1. Introduction

In the last years considerable attention has been paid to the problem of a bright state coupled to a manifold of dark background states. Dependent on the density of the coupled states the molecules are historically classified in terms of a small molecule or a large molecule [1]. In the small molecule limit the number of coupled dark states is very low. After excitation the molecule exhibits a single exponential decay with or without quantum beats and the quantum yield equals one. In the large molecule limit on the other hand, an excited molecule still decays exponentially. The quantum yield is however less than one as the high density of dark background states acts as a reservoir to which the energy flows irreversibly.

A molecule can exhibit characteristics of both limiting cases if several different types of background states are available. An example is pyrazine [2]. In this molecule the first excited singlet state is coupled to a sparse manifold of iso-energetic vibronically excited triplet states. This coupling results in mixed singlet–triplet eigenstates. These mixed singlet–triplet states are in turn coupled to a dense manifold of high

vibrationally excited states of the electronic ground state. This results in a low quantum yield.

It is interesting to investigate a continuous transition from the small molecule limit to the large molecule limit. An extensive mixing in the manifold of background states results in an averaging of the coupling matrix elements between the bright state and the dark states. A decrease in coupling matrix elements is also expected due to lower Franck–Condon factors. Also information about chaotic behaviour in the manifold of background states could be revealed. In this way information about chaotic behaviour could be derived [3].

A transition from the small molecule limit to the large molecule limit can be achieved by addition of one or more methyl groups [4] or by forming complexes [5]. In both ways the density of background states is increased. The density of background states can also be varied by a change in the excess energy over the vibrationless origin of the dark states. The density of vibronic states depends exponentially on the vibrational excess energy. We have therefore decided to study some vibronically excited states in pyrazine and pyrimidine with high resolution laser

spectroscopy. In this way we can also investigate a possible vibrational effect on the intersystem crossing. It has been shown for naphthalene that some vibrational modes exhibit a strongly enhanced intersystem crossing [6]. Also effects of intramolecular vibrational–rotational energy transfer (IVRET) may show up in the spectrum [7]. This would result in a scrambling of the rotational quantum number K' [8].

Pyrazine is a prototype for the coupling of a bright state to a set of dark states. Much information has been acquired over the years and a review is given in ref. [2]. The experimental data are interpreted in terms of a bright singlet state coupled to a set of nearly iso-energetic triplet states. The high resolution spectrum of the P(1)-branch of the 0_0^0 $S_1 \leftarrow S_0$ transition shows about 40 lines [9,10]. This number of lines in the P(1)-branch is an order of magnitude larger than an estimation based on the formula of Haarhoff [11]. The vibronically excited S_1 $6a^1$ state is located about 583 cm^{-1} above the vibrationless origin [12,13]. The state exhibits a relatively low quantum yield and the analysis of the biexponential decay suggests an increase in the number of coupled states by an order of magnitude [12]. We report here the high resolution spectrum of the $6a_0^1$ vibronic band of the $S_1 \leftarrow S_0$ electronic transition in pyrazine. A preliminary experimental spectrum is presented in ref. [13]. However, improvements in the experimental set-up allowed the recording of more detailed spectra.

Pyrimidine is quite similar to pyrazine. However, the high resolution spectrum of the 0_0^0 $S_1 \leftarrow S_0$ transition in pyrimidine appears less distorted [14]. This is due to both the lower density of dark states and the lower magnitude of the coupling matrix elements [14]. The vibrational dependence of the intersystem crossing up to 1300 cm^{-1} was investigated by Saigusa et al. [15]. They measured a smooth increase in the number of coupled states. Dispersed fluorescence spectra revealed no evidence for IVR up to a vibrational excess energy of 1000 cm^{-1} [16]. We have therefore measured the high resolution spectra of the $6a_0^1$ and the $6b_0^2$ vibronic bands of the $S_1 \leftarrow S_0$ electronic transition in pyrimidine. The $6a^1$ and $6b^2$ vibronically excited states are the two components of a Fermi resonance with excess energies of 613 cm^{-1} and 670 cm^{-1} [16].

2. Experimental

An extensive description of the molecular beam apparatus and the laser system has been given elsewhere [17]. Narrow band UV radiation is generated by intracavity frequency doubling in a single mode ring dye laser (a modified Spectra Physics 380D). Up to 15 mW of UV radiation with a band width of 3 MHz is obtained by using a 2 mm thick, Brewster cut LiIO$_3$ crystal. For relative frequency measurements a temperature stabilized sealed off Fabry–Pérot interferometer is used, while for absolute frequency measurements the iodine absorption spectrum was recorded simultaneously [18].

The molecular beam is formed by a continuous expansion of a mixture of pyrazine (pyrimidine) and argon through a nozzle with a diameter of 100 μm. Both the pyrimidine sample (Janssen Chimica, purity 99%) and the pyrazine sample (Janssen Chimica, purity 99 + %) were used at room temperature. The molecular beam is skimmed twice in a differential pumping system. In order to distinguish between stray laser light and the possibility of an overall present background fluorescence the molecular beam is chopped with 10 Hz. The rotational temperature in our molecular beam is typically 3 K.

Excitation of the molecules took place 30 cm from the nozzle orifice. The residual Doppler width in the beam is about 12 MHz and determined by the spatial filtering in the collection optics. The total undispersed fluorescence is imaged on a photomultiplier (EMI 9789QA). Data processing took further place with a standard photon counting system interfaced with a PDP11/23 + computer. In this way the full dynamical range of the spectrum could be used.

3. Results and analysis

3.1. Pyrimidine

With the experimental set-up described we have measured the laser induced fluorescence spectrum of two different vibronic bands of the $S_1 \leftarrow S_0$ electronic transition in pyrimidine, the $6a_0^1$ band at 315.6 nm and the $6b_0^1$ band at 315.0 nm. Both spectra consist of a Q-branch and P- and R-branches, clusters of lines separated by about 13 GHz. The observation of a

parallel transition is in accord with the symmetry assignments. In fig. 1 part of the $6a_0^1$ band is given. In fig. 2 the transitions to the excited state with rotational quantum number $J' = 3$ i.e. the P(4)- and R(2)-branch, are shown for the $6b_0^2$ vibronic band. It is recognizable, especially for the $K_{+1} = 1$ lines, that the rotational transitions to the same excited state consist of the same groups of lines. Comparison of these spectra of the two vibronic bands with the high resolution spectrum of the vibrationless $S_1 \leftarrow S_0$ electronic transition [14] clearly reveals that both the $6a_0^1$ band as well as the $6b_0^2$ band appear to be more distorted than the 0_0^0 band. Comparison of the transitions to the same excited state with rotational quantum numbers (J', K'_{-1}, K'_{+1}) is used to identify the lines in the spectrum. The deviations were in the order of the linewidth. The resemblance between the transitions to the same excited upper state proves that proves that the perturbation occurs in the excited vibronic state.

Except for the lines in the spectrum that could be identified with the vibronic transition in pyrimidine, both in the spectrum of the $6a_0^1$ band and in the spectrum of the $6b_0^2$ band unidentified lines appear throughout the whole investigated frequency range. The intensity of the strongest unidentified lines is about 4% of the strongest identified lines. A clear piling up of these unknown lines is visible in between the P- and R-branches. This is shown in the inset in fig. 1. There is no correspondence between the extra lines in the neighbourhood of a P-branch and the extra lines in the neighbourhood of the R-branch to the same excited state. Hence we conclude that these unidentified lines are not due to a perturbation in the excited vibronic state. Several alternative explanations are also rejected:

(i) A vibronically induced dipole moment might result in a hybrid band with some perpendicular band intensity. We have therefore simulated both an a-type transition as a b-type transition for these vibronic bands in pyrimidine. In the simulation we have used the rotational constants derived in the fit of the par-
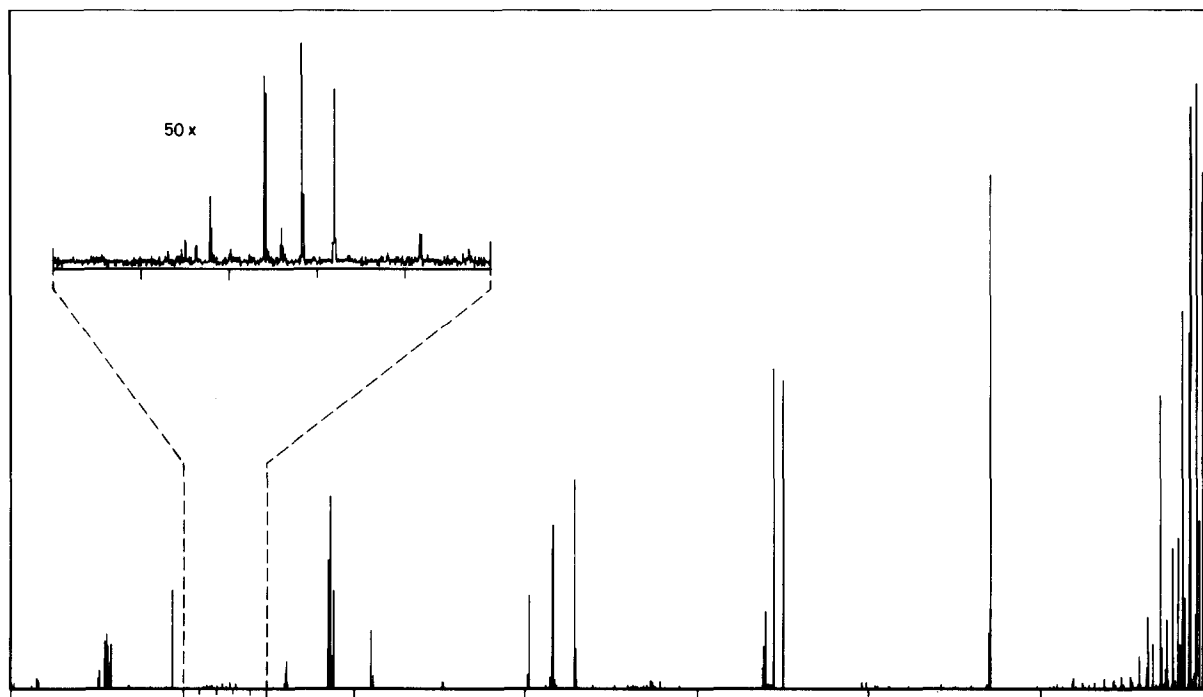

Fig. 1. Part of the laser induced fluorescence spectrum of the $6a_0^1$ vibronic band of the $S_1 \leftarrow S_0$ electronic transition in pyrimidine showing the P(5)- to Q-branch. The frequency is marked every 10 GHz and increases from left to right. The inset gives an exploded view of the spectrum showing the unidentified lines. Here the frequency is marked every GHz.
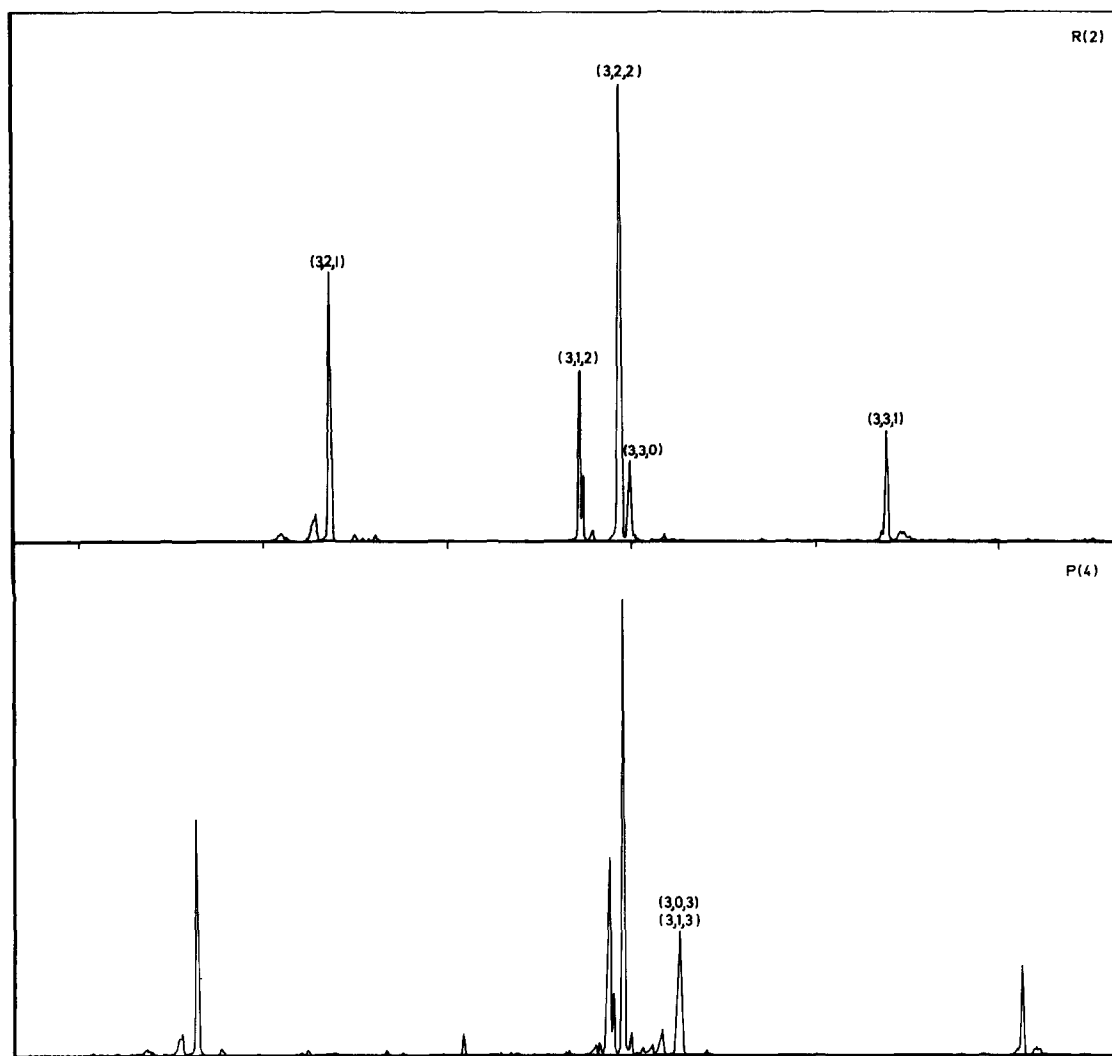
Fig. 2. The P(4) and R(2) transition of the $6b_0^2$ vibronic band of the $S_1 \leftarrow S_0$ electronic transition in pyrimidine. The frequency is marked every GHz and increases from left to right. The strongest lines are identified by the upper state rotational quantum numbers (J', K'_{-1}, K'_{+1}).

allel c-type band. No resemblance between the simulated spectrum and the unidentified lines was found however.

(ii) Transitions starting in highly excited rotational or excited vibrational states results in extra lines in between the branches. Therefore we have measured the part of the spectrum including the P(2)- and P(3)-branch with different backing pressures of the seeding gas argon. This results in spectra with dif-

ferent rotational temperatures between 2.5 and 4.5 K. The unidentified lines however exhibit the same pressure dependence as the identified lines in the P(2)- and P(3)-branch. Hence we conclude that these lines are not due to transitions from highly excited rotational or vibrational states. This observation also excludes complexes of pyrimidine.

(iii) Contributions from isotopically substituted species (e.g. ^{13}C) can also be ruled out, since this would

result in recognizable structures in the spectra similar to those of the most abundant isotopical species. Furthermore, one would expect a dependence of the intensities on the backing pressure, because in the case of an isotopically substituted species the observed transitions would certainly originate in higher rotational states.

The unidentified lines appear in both the $6a_0^1$ band and the $6b_0^2$ band and a clear piling up between the branches of pyrimidine is measured. However, no recognizable structure was found. Hence it is unlikely that the unidentified lines are due to a contamination of our pyrimidine sample. The origin of these lines remains therefore an enigma. The existence of these these lines does however not interfere with our analysis.

In order to detect a possible rotational dependence of the singlet–triplet coupling we have made a rotational assignment for the lines in the P(5)-branch to the R(3)-branch. We have fitted the spectrum to an asymmetric rotor Hamiltonian [19]. The center of gravity of the excitation intensity of the group of lines belonging to the same rotational transition is used. About 40 transitions were fitted to a parallel c-type band with axis-switching. The selection rules are in this case given by $(K''_{-1}, K''_{+1}) \rightarrow (K'_{-1}, K'_{+1}) =$ (ee)→(oe), (eo)→(eo), (oe)→(ee), (oo)→(oo) [20]. In the fit the rotational constants of the ground state were fixed to the values derived by microwave absorption spectroscopy [21] and only the rotational constants of the excited state and the center frequency of the rotationless vibronic transition were used as variables. Table 1 lists the obtained molecular constants. The standard deviation of the fit is about 30 MHz. In view of the interval of 300 MHz over which a group of lines belonging to the same rotational transition extends the fit is quite satisfactory. The rotational constants derived here are similar to the results for the 0_0^0 vibronic band [14].

We are now able to determine for some selected rotational states the number of coupled triplet states N, the density of the background triplet states ρ_T and the singlet–triplet coupling matrix elements V_{st}. However, some difficulties arise in this analysis. Since pyrimidine is an oblate near-symmetric rotor ($\kappa = 0.87$

in the electronic ground state and $\kappa = 0.74$ and 0.72 in the S_1 $6a^1$ and the S_1 $6b^2$ excited states respectively) several lines are overlapping. Furthermore, the extra unidentified lines in the spectra are disturbing. We have therefore restricted our analysis to the rotational transitions which were clearly separated in the spectra. Only those lines were taken into account which were present in both the P-branch and the R-branch to the same excited state. Exceptions to this rule are the lines in the P(2)-branch to the excited state with rotational quantum number $K'_{+1} = 1$. Although these lines have no counterpart in the R(0)-branch we have used them in our analysis, as these lines were clearly separated from all other lines.

In the calculation of the singlet–triplet coupling matrix elements V_{st} and the density of coupled triplet states ρ_T we use the procedure developed by Lawrance and Knight [22] to deconvolute the spectrum into the zero order singlet and triplet states. However, this method is in principle only applicable to a spectrum with known absorption intensities, whereas we have measured the laser induced fluorescence spectrum, i.e. a spectrum with excitation intensities. In case of a state $|i\rangle$ with decay rate γ_i the relation between the excitation intensity E_i and the absorption intensity A_i is given by

$$E_i = \beta \frac{A_i^2}{\gamma_i} .$$

In this equation β is a proportionality constant. Therefore we can derive the absorption spectrum from the laser induced fluorescence spectrum if the decay rates of the mixed singlet–triplet states are known [10]. However, as the decay rates are not known for the mixed singlet–triplet states in the $6a^1$ and $6b^2$ vibronic states in pyrimidine, two mutually exclusive approximations can be used:

(i) In case the decay rates of the zero-order triplet states are negligible with respect to the decay rate of the zero-order singlet state it is easy to show that the decay rate of the mixed singlet–triplet state is proportional to the intensity of that state [10]. Therefore the excitation intensity is proportional to the absorption intensity.

(ii) In case the decay rates of the zero-order triplet

Table 1

Rotational constants of the pyridine molecule in the electronic ground state S_0 and the $6a^1$ and $6b^2$ vibronic states of the singlet S_1 state. Also given are the center frequency ν_0 of the vibronic transition and the vibrational excess energy $\Delta\nu_0$ in the singlet S_1 state

		$6a^1$	$6b^2$
S_0	A" (MHz)	6276.86 [a]	
	B" (MHz)	6067.18 [a]	
	C" (MHz)	3084.49 [a]	
S_1	A' (MHz)	6321.6(0.5)	6294.7(0.5)
	B' (MHz)	5863.3(0.5)	5877.7(0.5)
	C' (MHz)	3029.4(0.5)	3040.5(0.5)
ν_0 (cm^{-1})		31686.029(0.004)	31741.934(0.004)
$\Delta\nu_0$ (cm^{-1})		613.371(0.008)	669.276(0.008)

[a] Ground state rotational constants were fixed to the values derived by microwave absorption spectroscopy [21]. The given errors in the rotational constants are the standard deviations of the fit.

states are comparable to the decay rate of the zero-order singlet state we can make the approximation that the lifetimes of all mixed singlet–triplet states are equal. In this case the absorption intensity is proportional to the square root of the excitation intensity.

The measured lifetime of the strongest lines in the P(1)-branch of the 0_0^0 $S_1 \leftarrow S_0$ electronic transition in pyrazine showed that there is no clear correspondence between the intensity of the transition to the mixed singlet–triplet state and the decay rate of the this state. Also the deconvolution procedure applied to the eigenstates revealed that the decay rates of the zero-order triplet states are comparable to the decay rate of the zero-order singlet state [10]. Hence we have set in our analysis the decay rates of the measured mixed singlet–triplet states in the $6a_0^1$ and the $6b_0^2$ vibronic transitions in pyrimidine all equal. We have however applied both the deconvolution procedure with an assumed constant lifetime and the deconvolution procedure with an assumed lifetime proportional to the intensity for some excited rotational states. The differences between the results of the two deconvolution procedures were minor. Hence the conclusions derived from the deconvolution of the spectra are not influenced by the assumption of the equal lifetimes for the different mixed singlet–triplet states.

With the assumed constant lifetime and the measured fluorescence intensities we are now able to deconvolute the spectrum for some selected rotational states into the zero-order singlet and triplet states. The result of the deconvolution procedure is given in ta-

ble 2. The density of coupled triplet states ρ_T is here defined for a set of triplet states $\{|T_1\rangle \cdots |T_N\rangle\}$ with energies $\{E_1 \cdots E_N\}$ by

$$\rho_T = \frac{N-1}{E_N - E_1}.$$

The measured density of states ρ_T is an underestimation of the real density due to the finite signal to noise ratios in the spectra and the finite line width.

3.2. Pyrazine

With the experimental set-up described we have also measured the $6a_0^1$ vibronic band of the $S_1 \leftarrow S_0$ vibronic transition in pyrazine at 317.9 nm. The vibrational excess energy in the excited singlet state is 583 cm^{-1}. The spectrum consists of a Q-branch with clearly separated P- and R-branches. The spectrum corresponds to a c-type transition in an oblate near-symmetric rotor, in accord with the symmetry assignments. In fig. 3 the P(1)-branch is depicted. In between the branches no broad background fluorescence is observed. This means with the present signal to noise ratio that a possible overall present broad band fluorescence [12,23] is at least a factor 1000 weaker compared to the strong lines in the P(1)-branch.

In order to determine whether there are any lines present which do not belong to the $6a_0^1$ vibronic band of pyrazine we have compared the R(0)-branch with the P(2)-branch. All lines present in the R(0)-branch have their counterpart in the P(2)-branch. Hence we conclude that all lines measured in our laser induced

Table 2
The number of coupled states N, the density of coupled states ρ_T and the average coupling matrix element $\langle V_{st} \rangle$ for some selected rotational states (J', K'_{-1}, K'_{+1}) of the S_1 6a^1 and the S_1 6b^2 vibronic states in pyrimidine

	J'	K'_{-1}	K'_{+1}	N	ρ_T (/cm^{-1})	$\langle V_{st} \rangle$ (MHz)
6a^1	1	0	1	5	41	17
	1	1	1	0		
	1	1	0	2	19	67
	2	1	1	2	3	30
	2	2	1	5	24	13
	2	2	0	6	8	42
	3	2	1	7	25	15
	3	3	1	6	11	37
	4	2	2	3	12	40
	4	3	1	7	22	25
	4	4	1	2	40	19
6b^2	1	0	1	5	16	22
	1	1	1	5	8	62
	1	1	0	5	4	54
	2	1	1	7	14	38
	2	2	1	10	16	46
	2	2	0	3	7	33
	3	2	1	11	19	36
	3	3	1	12	16	35
	4	2	2	5	26	19
	4	3	1	5	29	18
	4	4	1	12	16	30

fluorescence spectrum belong to the 6a$_0^1$ vibronic band in pyrazine.

Even in the R(0)-branch many lines are overlapping. Therefore we have restricted our analysis to the P(1)-branch. A list of the measured frequencies and intensities is given in table 3. We have applied the procedure of Lawrance and Knight [22] to deconvolute the spectrum into the zero-order singlet and triplet states. In this procedure we have assumed that the decay rates of all the mixed singlet–triplet states are equal. The result of this deconvolution procedure is given in table 4. The singlet position is calculated at +194 MHz. This value corresponds to the center of gravity of the absorption intensities.

4. Discussion

It has been shown for the 6a$_0^1$ and the 6b$_0^2$ vibronic bands in pyrimidine that each rotational transition

corresponds to a well-defined group of lines. As these groups of lines are entirely different for the transitions to the states with different K'_{-1}, K'_{+1} quantum numbers, it is concluded that the rotational quantum numbers K'_{-1}, K'_{+1} are still valid in the 6a^1 and 6b^2 vibronic states in pyrimidine. In case of an extensive K'-scrambling in the excited state the transitions to states with the same rotational quantum number J' but different rotational quantum number K' would consist of identical groups of lines but with different relative intensities. This result shows that there is neither a direct coupling within the excited singlet state nor an indirect coupling via an intermediate triplet state in pyrimidine up to 670 cm^{-1} of vibrational excess energy. This result is not surprising as two nearby excited rotational states cannot interact due to different symmetry species [the rotational symmetry in the excited S_1 state is A$_1$ in case $(K_{-1}, K_{+1}) = $(e, e), A$_2$ in case $(K_{-1}, K_{+1}) = $(e, o), B$_1$ in case $(K_{-1}, K_{+1}) = $(o, o) and B$_2$ in case $(K_{-1}, K_{+1}) = $(o, e)]. Rotational states with the same symmetry have large energy separations with respect to the typical singlet–triplet coupling matrix elements of 50 MHz. The fact that there is no coupling within the singlet state justifies the use of the deconvolution procedure as this procedure is only applicable to a single bright state coupled to a set of dark states.

The results of the deconvolution procedure for the two vibronic bands in pyrimidine as listed in table 2 indicate that neither the number of coupled states N nor the average coupling matrix elements $\langle V_{st} \rangle$ systematically depend on the rotational quantum numbers (J', K'_{-1}, K'_{+1}). In case of an extensive K-scrambling in the set of background states the number of coupled states would increase linearly with the rotational quantum number J'. Hence we conclude that there is no extensive K-scrambling in the triplet state of pyrimidine at 3200 cm^{-1} excess energy. The absence of a rotational effect on the coupling matrix elements V_{st} indicates an absence of a Coriolis induced inter-system crossing in pyrimidine. It should be noted however that this result is not in contradiction with the rotational dependence of the decay process of the mixed singlet–triplet eigenstates in the vibrationless excited singlet state [14].

We can compare the measured density of coupled states ρ_T with the density of vibronic states calculated with the formula of Haarhoff [11]. In the calculation
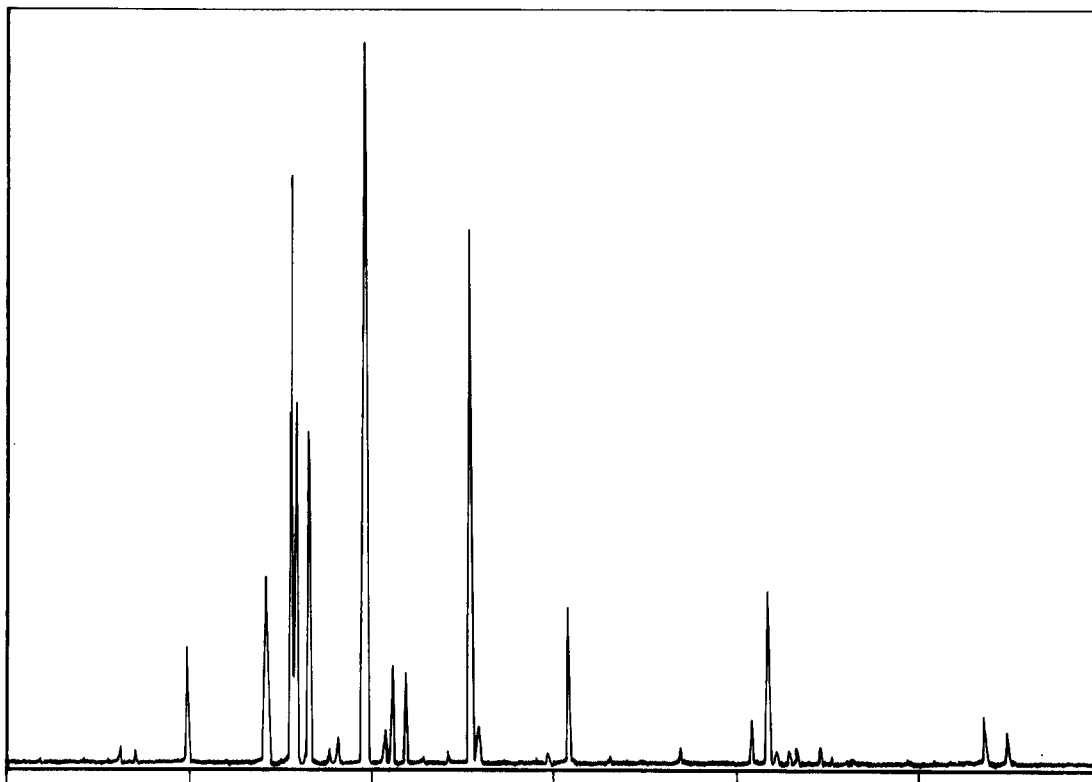
Fig. 3. The P(1)-branch of the $6a_0^1$ vibronic band of the $S_1 \leftarrow S_0$ electronic transition in pyrazine. The frequency is marked every GHz and increases from left to right.

the ground state vibrational frequencies are used [16]. This probably results in an underestimation of the calculated density of states since ground state frequencies tend to be higher. A singlet–triplet gap of 2543 cm^{-1} is assumed [24]. The calculation results in a density of vibronic states $\rho_T^v = 6$ states per cm^{-1} at a triplet excess energy of 3200 cm^{-1}.

To calculate the density of coupled triplet states the selection rules for spin–orbit coupling have to be considered. Since direct spin–orbit coupling is forbidden between singlet and triplet states of the same electronic configuration we have to consider second-order spin–orbit coupling. The matrix elements and selection rules for vibronically induced spin–orbit coupling and rotationally induced spin–orbit coupling are derived by Stevens and Brand [25].

In case of vibronically induced spin–orbit coupling vibrations of the symmetry species a_2, b_1 and b_2 in

the T_1 states can couple to the excited singlet state. The rotational selection rules (symmetric top limit) are $\Delta J = 0$, $\Delta N = 0$, ± 1 and $\Delta K = 0$ (if the symmetry species of the vibration is b_2) and $\Delta J = 0$, $\Delta N = 0$, ± 1 and $\Delta K = \pm 1$ (if the symmetry species of the vibration is a_2 or b_1). Hence an estimation of the calculated density of triplet states coupled via vibrationally induced spin–orbit coupling amounts to $\rho_T = 20$ states per cm^{-1}.

In case of rotationally induced spin–orbit coupling vibrations of the symmetry species a_1 can couple to the excited singlet state with the rotational selection rules $\Delta J = 0$, $\Delta N = 0$, ± 1 and $\Delta K = 0$, ± 2 (symmetric top limit). Hence the calculated density of triplet states coupled via rotationally induced spin–orbit coupling amounts to $\rho_T = 14$ states per cm^{-1}.

The measured total density of states is on the order of 20 states per cm^{-1}, in good agreement with the calculation.

Table 3

Observed frequencies and intensities of the transitions in the P(1)-branch of the S_1 (6a^1)←S_0 vibronic transition in pyrazine. Frequencies are given relative to the center of gravity of the excitation intensity

frequency (MHz)	intensity	frequency (MHz)	intensity
−2087	52	149	142
−1848	57	268	5829
−1654	127	317	435
−1566	134	695	113
−1280	1277	811	1689
−877	66	1036	68
−855	2076	1416	158
−837	184	1809	500
−711	6440	1898	1893
−689	3979	1944	137
−620	3618	2017	155
−499	163	2059	177
−456	301	2183	183
−308	7883	2245	62
−198	383	2369	61
−158	1078	3085	515
−83	1000	3099	240
15	54	3215	372

Table 4

Calculated triplet state positions and singlet–triplet coupling matrix elements V_{st} for the $J'=0$ state of the S_1 (6a^1) vibronic state of pyrazine. The singlet position is calculated at 194 MHz. The positions are given relative to the center of gravity of the excitation intensity. Also given are the density of triplet states ρ_T and the average coupling matrix element $\langle V_{st}\rangle$.

frequency (MHz)	V_{st} (MHz)	frequency (MHz)	V_{st} (MHz)
−2074	145	182	194
−1836	129	308	53
−1640	126	660	277
−1548	161	750	244
−1237	209	1020	162
−875	20	1364	404
−843	36	1626	651
−817	106	1840	155
−700	28	1935	71
−647	80	1999	132
−523	150	2046	95
−477	110	2161	166
−409	200	2235	102
−226	136	2356	136
−179	81	2962	570
−106	109	3093	33
6	97	3188	172
109	251		

$\rho_T = 194$ states per cm^{-1}

$\langle V_{st}\rangle = 178$ MHz

The results for the 6a$_0^1$ and the 6b$_0^2$ vibronic bands in pyrimidine show no marked difference. As the vibrational wave functions are extensively mixed due to the Fermi resonance [16], this result is not surprising. A comparison of the results for the 0$_0^0$ band and the results for the 6a$_0^1$ and 6b$_0^2$ vibronic bands is hampered by the low dynamical range of the spectra of the 0$_0^0$ band [14]. However, the coupling matrix elements are the same order of magnitude in these three states. Hence we conclude that there is no strong vibrational effect on the intersystem crossing in pyrimidine for the lower vibronic states considered here.

The spectrum of the 6a$_0^1$ vibronic band in pyrazine clearly reveals that (K'_{-1}, K'_{+1}) are still valid quantum numbers in the excited state at a vibrational excess energy of 583 cm^{-1}. Therefore the use of the deconvolution procedure is justified. We are now able to compare the results for the $(J', K'_{-1}, K'_{+1}) = (0, 0, 0)$ rotational state in the S_1 6a^1 state, as listed in table 4, with the results for the $(J', K'_{-1}, K'_{+1}) = (0, 0, 0)$ rotational state in the vibrationless S_1 state, as given in ref. [10]. However, the signal to noise ratio for the P(1)-branch was better in the 0$_0^0$ vibronic

band than in the 6a$_0^1$ vibronic band. This means that more weak lines are visible in the 0$_0^0$ vibronic band. Furthermore, the deconvolution procedure for the vibrationless S_1 state was performed with the known decay rates of the mixed singlet–triplet states. In order to compare the results for the different vibronic states we have repeated the deconvolution procedure for the P(1) branch of the 0$_0^0$ band. In this new deconvolution of the spectrum only the 14 strongest lines with an intensity of more than 0.6% of the strongest line were taken into account, in accord with the signal to noise ratio of the 6a$_0^1$ band. A constant lifetime was used for the excited mixed singlet–triplet states.

The result for the measured density of triplet states is $\rho_T = 82$ states per cm^{-1} in the vibrationless excited state and $\rho_T = 194$ states per cm^{-1} in the 6a^1 excited states. This corresponds with an increase in the density of triplet states with a factor 2.4. A calculation using the ground state frequencies [16] results in an

increase in the density of background states with a factor of 2.7, in good agreement with the experimental value.

The calculation resulted in a density of vibronic triplet states $\rho_T^v = 35$ states per cm^{-1} at a triplet vibrational excess energy of 4056 cm^{-1} and $\rho_T^v = 93$ states per cm^{-1} at a triplet vibrational excess energy of $4056 + 582$ cm^{-1}. These calculated densities are somewhat less than results reported elsewhere [2,27]. With the selection rules for indirect spin–orbit coupling [25] we deduce a calculated density of coupled triplet states to the $(J', K'_{-1}, K'_{+1}) = (0, 0, 0)$ rotational singlet state as $\rho_T = 4$ states per cm^{-1} at a vibrational excess energy of 4056 cm^- and $\rho_T = 12$ states per cm^{-1} at a vibrational excess energy of $4056 + 582$ cm^{-1}.

This result is two orders of magnitude less then the measured density of states. Since the density of triplet states is measured for the $J' = 0$ state we cannot explain this large discrepancy by the assumption of a resolved hyperfine structure [27]. The large discrepancy between the calculated density of states and the measured density of states suggests therefore a coupling within the triplet manifold resulting in a relaxation of the singlet–triplet selection rules. Such an interstate coupling is also assumed in the explanation of the high resolution magnetic field spectra of the pyrimidine molecule [14].

The average coupling strength is given by $\langle V_{st} \rangle = 214$ MHz in the vibrationless excited state and $\langle V_{st} \rangle = 178$ MHz in the $6a^1$ excited state. This small decrease in coupling constant can be attributed to a diminishing Franck–Condon overlap between the bright singlet state and the vibronically excited triplet states.

It is interesting to determine whether the vibrational states in the triplet state are completely mixed. In case of an extensive mixing we expect an averaging of the coupling matrix elements. As a measure of the degree of mixing we have calculated the number

$$\frac{1}{N} \sum \frac{\langle V_{st} - \langle V_{st} \rangle \rangle^2}{\langle V_{st} \rangle^2} .$$

This number amounts to 0.54 in the vibrationless excited state and 0.65 in the $6a^1$ excited state. We conclude that the increase in vibrational excess energy with 583 cm^{-1} does not result in an additional mix-

ing of the vibrational wave functions of the vibronic background states. Hence the variation in the singlet–triplet coupling matrix elements is determined by the Franck–Condon overlap between the bright singlet state and the dark background states.

References

[1] F. Lahmani, A. Tramer and C. Tric, J. Chem. Phys. 60 (1974) 4431.
[2] J. Kommandeur, W.A. Majewski, W.L. Meerts and D.W. Pratt, Ann. Rev. Phys. Chem. 38 (1987) 433.
[3] S.L. Coy and K.K. Lehmann, Phys. Rev. A 36 (1987) 404.
[4] K. Uchida, I. Yamazaki and H. Baba, Chem. Phys. 35 (1978) 91.
[5] H. Abe, Y. Ohyanagi, M. Ichijo, N. Mikami and M. Ito, J. Phys. Chem. 89 (1985) 3512.
[6] T. Suzuki, M. Sato, N. Mikami and M. Ito, Chem. Phys. Letters 127 (1986) 292;
P. Uijt de Haag and W.L. Meerts, Chem. Phys. 135 (1989) 139.
[7] G.M. Nathanson and G.M. McClelland, J. Chem. Phys. 84 (1986) 3170.
[8] P.J. de Lange, B.J. van der Meer, K.E. Drabe, J. Kommandeur, W.L. Meerts and W.A. Majewski, J. Chem. Phys. 86 (1987) 4004.
[9] B.J. van der Meer, H.T. Jonkman, J. Kommandeur, W.L. Meerts and W.A. Majewski, Chem. Phys. Letters 92 (1982) 565.
[10] W.M. van Herpen, W.L. Meerts, K.E. Drabe and J. Kommandeur, J. Chem. Phys. 86 (1987) 4396.
[11] P.C. Haarhoff, Mol. Phys. 7 (1963) 101.
[12] A. Amirav, Chem. Phys. 126 (1988) 365.
[13] B.J. van der Meer, Thesis (1985).
[14] W.L. Meerts and W.A. Majewski, Laser Chem. 5 (1986) 339;
J.A. Konings, W.A. Majewski, Y. Matsumoto, D.W. Pratt and W.L. Meerts, J. Chem. Phys. 89 (1988) 1813.
[15] H. Saigusa, A.K. Jameson and E.C. Lim, J. Chem. Phys. 79 (1983) 5228.
[16] A.E.W. Knight, C.M. Lawburgh and C.S. Parmenter, J. Chem. Phys. 63 (1975) 4336.

[17] W.A. Majewski and W.L. Meerts, J. Mol. Spectry. 104 (1984) 271;
W.M. van Herpen, Thesis (1988).

[18] S. Gerstenkorn and P. Luc, Atlas du Spectroscopie d'Absorption de la Molecule d'Iode (Centre National de la Recherche Scientifique, 1978); Rev. Phys. Appl. 14 (1979) 791.

[19] J.K.G. Watson, J. Chem. Phys. 46 (1967) 1935; 48 (1968) 4517.

[20] R.E. Smalley, L.H. Wharton, D.H. Levy and D.W. Chandler, J. Mol. Spectry. 66 (1977) 375.

[21] G.L. Blackman, R.D. Brown and F.R. Burden, J. Mol. Spectry. 35 (1970) 444.

[22] W.D. Lawrance and A.E.W. Knight, J. Phys. Chem. 89 (1985) 917.

[23] A. Amirav, Chem. Phys. 108 (1986) 403.

[24] T. Takemura, K. Uchida, M. Fujita, Y. Shindo, N. Suzuki and H. Baba, Chem. Phys. Letters 73 (1980) 12.

[25] C.G. Stevens and J.C.D. Brand, J. Chem. Phys. 58 (1973) 3324.

[26] G. Herzberg, Molecular Spectra and Molecular Structure, Vol. 3 (Van Nostrand Reinhold, New York, 1966).

[27] W. Siebrand, W.L. Meerts and D.W. Pratt, J. Chem. Phys. 90 (1989) 1313.